Higher-order rogue wave solutions of the Kundu–Eckhaus equation

2014 Phys. Scr. 89 095210

(http://iopscience.iop.org/1402-4896/89/9/095210)

IOP Publishing | Royal Swedish Academy of Sciences Physica Scripta
Phys. Scr. 89 (2014) 095210 (15pp) doi:10.1088/0031-8949/89/9/095210

Higher-order rogue wave solutions of the Kundu–Eckhaus equation

Xin Wang[1], Bo Yang[1], Yong Chen[1] and Yunqing Yang[2]

[1] Shanghai Key Laboratory of Trustworthy Computing, East China Normal University, Shanghai 200062, People's Republic of China
[2] School of Mathematics, Physics and Information Science, Zhejiang Ocean University, Zhoushan 316004, People's Republic of China

E-mail: ychen@sei.ecnu.edu.cn

Received 25 May 2014, revised 3 July 2014
Accepted for publication 9 July 2014
Published 20 August 2014

Abstract

In this paper, we investigate higher-order rogue wave solutions of the Kundu–Eckhaus equation, which contains quintic nonlinearity and the Raman effect in nonlinear optics. By means of a gauge transformation, the Kundu–Eckhaus equation is converted to an extended nonlinear Schrödinger equation. We derive the Lax pair, the generalized Darboux transformation, and the Nth-order rogue wave solution for the extended nonlinear Schrödinger equation. Then, by using the gauge transformation between the two equations, a concise unified formula of the Nth-order rogue wave solution with several free parameters for the Kundu–Eckhaus equation is obtained. In particular, based on symbolic computation, explicit rogue wave solutions to the Kundu–Eckhaus equation from the first to the third order are presented. Some figures illustrate dynamic structures of the rogue waves from the first to the fourth order. Moreover, through numerical calculations and plots, we show that the quintic and Raman-effect nonlinear terms affect the spatial distributions of the humps in higher-order rogue waves, although the amplitudes and the time of appearance of the humps are unchanged.

Keywords: rogue wave, Kundu–Eckhaus equation, generalized Darboux transformation

1. Introduction

The popularity of rogue waves (also known as freak waves, monster waves, killer waves, mad- or rabid-dog waves and similar names) has grown rapidly in recent years [1–3]. The term 'rogue waves' was originally used to describe mysterious giant ocean waves, a horrible phenomenon that can lead to water walls taller than 20–30 m and that represents a catastrophe for ships, offshore oil platforms, and so on [1]. A wave can be assigned to this category when its height is two or three times larger than the background crest and appears from nowhere and disappears without a trace [4]. In addition to being found in the deep ocean, rogue waves have been discovered in other fields, among them optics [2, 3], capillary flow [5], superfluidity [6], Bose–Einstein condensates [7], plasma physics [8], the atmosphere [9], and even finance [10].

It is well known that the standard nonlinear Schrödinger (NLS) equation

$$\mathrm{i}u_t + u_{xx} + 2|u|^2 u = 0, \tag{1}$$

which contains group velocity dispersion and self-phase modulation, is a basic model that describes optical soliton propagation in Kerr media [11]. The complete integrability and multi-soliton solutions, breather solutions, and various types of rogue wave solutions associated with the NLS equation have been widely reported by many authors [12–21]. Nevertheless, in optic fiber communications systems, one always has to increase the intensity of the incident light field to produce ultrashort (femtosecond) optical pulses [37]. In this case, the simple NLS equation is inadequate to accurately describe the phenomena, and higher-order nonlinear terms, such as third-order dispersion, self-steepening, and self-frequency shift, must be taken into account [23–29].

In this paper, we consider the Kundu–Eckhaus (KE) equation, which contains quintic nonlinearity and the Raman effect in nonlinear optics [30],

$$\mathrm{i}u_t + u_{xx} + 2|u|^2u + 4\beta^2|u|^4u - 4\mathrm{i}\beta\left(|u|^2\right)_x u = 0, \quad (2)$$

where $u(x, t)$ is the complex smooth envelop function and the subscripts x and t are spatial and temporal partial derivatives. β is a real constant, β^2 is the quintic nonlinear coefficient, and the last term represents the Raman effect, which is responsible for the self-frequency shift. The KE equation was proposed by Kundu when he studied the gauge connections among some generalized Landau–Lifshitz and higher-order NLS systems; it adequately describes the propagation process of ultrashort optical pulses in nonlinear optics [31] and examines the stability of the Stokes wave in weakly nonlinear dispersive matter waves [32]. A series of important results related to equation (2) have been obtained, such as the gauge connections between equation (2) and other soliton equations [30], the Lax pair and the Hamiltonian structure [33], and soliton solutions through the Darboux transformation [34–36], based on an extended Ablowitz–Kaup–Newell–Segur (AKNS) spectral problem, Zhaqilao constructed a generalized Darboux transformation (DT) for equation (2), and the explicit first-order rogue wave solution and the modulus form of the second-order rogue wave solution were given. Moreover, very recently, Zhao, Liu, and Yang revisited the first-order rogue wave solution to equation (2) through the method of transforming the Lax pair matrix to the Jordan form, and some dynamic properties of the rogue wave solution were analyzed [38].

Generalization to even higher-order solutions is difficult and not trivial, as is remarked in [20]. Recently there has been a notable surge in interest in classifying the hierarchy of higher-order rogue wave solutions to NLS-type [39–41]. In general, higher-order rogue wave solutions can be classified into fundamental, triangular, pentagram, heptagram, and even more complicated patterns. However, to our knowledge, there are no reports regarding higher-order rogue wave solutions to equation (2). The generalized DT based on the aforementioned extended AKNS spectral problem cannot be used directly to generate higher-order rogue wave solutions because, in every iterative process, it is necessary to solve two complicated partial differential equations to get the concrete expressions of α_j ($j = 1, 2, \ldots$), and when $j \geqslant 3$, the solution procedure is very difficult and the higher-order (second-order, third-order, etc) rogue wave solutions cannot be explicitly derived, as is remarked in [37]. Owing to the extensive applications of equation (2), it is essential to find an effective formula to generate higher-order rogue wave solutions for it. By studying the dynamic properties of higher-order rogue waves, one can have a more comprehensive understanding of the influencing mechanism produced by the quintic and Raman-effect nonlinear terms on rogue waves in nonlinear optics.

The aim of our paper is to construct higher-order rogue wave solutions to equation (2) and to discuss their dynamic distributions by choosing different values of the free parameters. Instead of studying rogue wave solutions for equation (2) directly, we concentrate on the solution to an extended NLS equation that is gauge equivalent to it, that is,

$$\begin{aligned}&\mathrm{i}q_t + q_{xx} + 2|q|^2q + 2\mathrm{i}\beta\left(|q|^2q_x - q^2q_x^*\right)\\ &\quad -2\beta q\int\left(|q|^2\right)_t dx = 0,\end{aligned} \quad (3)$$

whose Lax pair is the standard AKNS spectral problem [34, 42] together with the corresponding auxiliary problem (given hereafter). When $\beta = 0$, the preceding equation is reduced to the standard NLS equation. In this paper, we first construct the generalized DT [21, 43–47] and the Nth-order rogue wave solution for equation (3). Then, by means of the gauge transformation between the two equations, a concise unified formula for an Nth-order rogue wave solution for equation (2) is derived. Furthermore, the compact $2N \times 2N$ determinant representation of the formula is given. As an application, based on symbolic computation [48–50], explicit rogue wave solutions to equation (2), from the first to the third order, are presented. Some figures are used to illustrate dynamic structures of the rogue waves from the first to the fourth order. Moreover, the influences produced by the small parameter β on the higher-order rogue waves are discussed in detail with the help of numerical calculations and plots. We find that by taking different values of the small parameter β, the spatial distributions of the humps in higher-order rogue waves can be affected, whereas the amplitudes and the time of appearance of the humps are unchanged.

The outline of our paper is as follows. In section 2, we give the gauge transformation between equations (2) and 3 and derive the Lax pair of equation (3). In section 3, a generalized DT is constructed, and a concise unified formula for an Nth-order rogue wave solution for equation (2) is given. In section 4, some explicit rogue wave solutions, figures, and numerical calculations are presented. The final section is a discussion section.

2. Gauge transformation and Lax pair

In this section, we present the gauge transformation between equations (2) and (3) and derive the Lax pair of equation (3) by using the AKNS procedure [42]. We start from the extended AKNS spectral problem [33]

$$\begin{aligned}&y_x = Uy, \quad y = \begin{pmatrix} y_1(x, t) \\ y_2(x, t) \end{pmatrix},\\ &U = \begin{pmatrix} -\mathrm{i}\zeta + \mathrm{i}\beta|u|^2 & u \\ -u^* & \mathrm{i}\zeta - \mathrm{i}\beta|u|^2 \end{pmatrix},\end{aligned} \quad (4)$$

with the auxiliary problem

$$\begin{aligned}&y_t = Vy,\\ &V = \begin{pmatrix} V_{11} & 2u\zeta + \mathrm{i}u_x + 2\beta|u|^2u \\ -2u^*\zeta + \mathrm{i}u_x^* - 2\beta|u|^2u^* & -V_{11} \end{pmatrix},\end{aligned} \quad (5)$$

where

$$V_{11} = -2\mathrm{i}\zeta^2 + \mathrm{i}|u|^2 + \beta\left(uu_x^* - u_x u^*\right) + 4\mathrm{i}\beta^2|u|^4,$$

u is the potential, and ζ is a constant spectral parameter. By making use of the compatibility condition $U_t - V_x + UV - VU = 0$, one can directly obtain equation (2). Next, according to [51] (section 1.4) and [52] (section 4.2), we know that the following transformation,

$$y = \begin{pmatrix} \exp\left(\mathrm{i}\beta\int|q|^2dx\right) & 0 \\ 0 & \exp\left(-\mathrm{i}\beta\int|q|^2dx\right)\end{pmatrix}\Psi, \quad (6)$$

$$u = q\exp\left(2\mathrm{i}\beta\int|q|^2dx\right), \quad (7)$$

converts the extended AKNS spectral problem (4) to the standard AKNS spectral problem. Here $q = q(x, t)$ is the new potential and $\Psi = (\psi(x, t), \phi(x, t))^T$ is the new spectral function. Hence, we have the following proposition.

Proposition 1. *From a known solution q of the extended NLS equation (3), the explicit formula (7) gives a new special solution to the KE equation, and the Lax pair of the extended NLS equation (3) reads*

$$\Psi_x = \hat{U}\Psi,\ \hat{U} = \begin{pmatrix} -\mathrm{i}\zeta & q \\ -q^* & \mathrm{i}\zeta \end{pmatrix}, \quad (8)$$

$$\Psi_t = \hat{V}\Psi,\ \hat{V} = \begin{pmatrix} \hat{V}_{11} & 2\zeta q + \mathrm{i}q_x \\ -2\zeta q^* + \mathrm{i}q_x^* & -\hat{V}_{11} \end{pmatrix}, \quad (9)$$

where

$$\hat{V}_{11} = -2\mathrm{i}\zeta^2 + \mathrm{i}|q|^2 + \beta\left(qq_x^* - q_x q^*\right) - \mathrm{i}\beta\int\left(|q|^2\right)_t dx.$$

Proof. By directly substituting (7) into the KE equation, together with the extended NLS equation (3), one can show that the equation holds. Then, substituting (6) into (4) and (5), and using the AKNS procedure, we can derive the linear spectral problem (8) and (9). Furthermore, it is easy to verify that the extended NLS equation (3) can be exactly reproduced from the compatibility condition $\hat{U}_t - \hat{V}_x + \hat{U}\hat{V} - \hat{V}\hat{U} = 0$.

Remark 1. According to proposition 1, we see that equations (2) and (3) are gauge equivalent to each other. Therefore, considering the complete integrability of the KE equation, the extended NLS equation (3) can also be regarded as completely integrable.

3. Generalized Darboux transformation

In this section, by resorting to the Lax pair (8) and (9), we first construct the classical DT and the generalized DT for equation (3). Let $\Psi_1 = (\psi_1, \phi_1)^T$ be a solution to the Lax pair equations (8) and (9) at $q = q[0]$ and $\zeta = \zeta_1$; subsequently, the classical DT of equation (3) can be defined as

$$\Psi[1] = T[1]\Psi,\ T[1] = \zeta I - H[0]\Lambda_1 H[0]^{-1}, \quad (10)$$

$$q[1] = q[0] - 2\mathrm{i}\left(\zeta_1 - \zeta_1^*\right)\frac{\psi_1[0]\phi_1[0]^*}{\left(\left|\psi_1[0]\right|^2 + \left|\phi_1[0]\right|^2\right)}, \quad (11)$$

where $\psi_1[0] = \psi_1$, $\phi_1[0] = \phi_1$,

$$I = \begin{pmatrix} 1 & 0 \\ 0 & 1 \end{pmatrix},\ H[0] = \begin{pmatrix} \psi_1[0] & -\phi_1[0]^* \\ \phi_1[0] & \psi_1[0]^* \end{pmatrix},\ \Lambda_1 = \begin{pmatrix} \zeta_1 & 0 \\ 0 & \zeta_1^* \end{pmatrix}.$$

Now let $\Psi_l = (\psi_l, \phi_l)^T$ $(1 \leqslant l \leqslant N)$ be a solution to the Lax pair equations (8) and (9) for $q = q[0]$ and $\zeta = \zeta_l$. Repeating the above process N times, we get the N-step DT of equation (3),

$$\Psi[N] = T[N]T[N-1]\ldots T[1]\Psi,\ T[l] = \zeta I - H[l-1]\Lambda_l H[l-1]^{-1}, \quad (12)$$

$$q[N] = q[N-1] - 2\mathrm{i}\left(\zeta_N - \zeta_N^*\right) \times \frac{\psi_N[N-1]\phi_N[N-1]^*}{\left(\left|\psi_N[N-1]\right|^2 + \left|\phi_N[N-1]\right|^2\right)}, \quad (13)$$

where $(\psi_l[l-1], \phi_l[l-1])^T = \Psi_l[l-1]$,

$$\Psi_l[l-1] = \left(T[l-1]T[l-2]\ldots T[1]\right)\Big|_{\zeta=\zeta_l}\Psi_l,$$

$$H[l-1] = \begin{pmatrix} \psi_l[l-1] & -\phi_l[l-1]^* \\ \phi_l[l-1] & \psi_l[l-1]^* \end{pmatrix},$$

$$\Lambda_l = \begin{pmatrix} \zeta_l & 0 \\ 0 & \zeta_l^* \end{pmatrix},\ 1 \leqslant l \leqslant N.$$

Thus, in terms of the above facts, we can construct the generalized DT for equation (3). Suppose $\Psi_1(\zeta_1 + \delta)$ is a basic solution to the Lax pair equations (8) and (9) where $q = q[0]$ and $\zeta = \zeta_l + \delta$; here δ is a small parameter. We assume that the vector function Ψ_1 can be expanded as a Taylor series at $\delta = 0$:

$$\Psi_1 = \Psi_1^{[0]} + \Psi_1^{[1]}\delta + \Psi_1^{[2]}\delta^2 + \Psi_1^{[3]}\delta^3 + \ldots + \Psi_1^{[N]}\delta^N + \ldots, \quad (14)$$

where $\Psi_1^{[k]} = \left(\psi_1^{[k]}, \phi_1^{[k]}\right)^T = \lim_{\delta\to 0}\frac{1}{k!}\frac{\partial^k\Psi_1}{\partial\delta^k}$, $k = 0, 1, 2, \ldots$.

It is apparent that $\Psi_1^{[0]}$ is a special solution to the Lax pair equations (8) and (9) for $q = q[0]$ and $\zeta = \zeta_1$, so the first-step generalized DT can be spontaneously given.

(1) The first-step generalized DT follows.

$$\Psi[1] = T[1]\Psi,\ T[1] = \zeta I - H[0]\Lambda_1 H[0]^{-1}, \quad (15)$$

$$q[1] = q[0] - 2\mathrm{i}\left(\zeta_1 - \zeta_1^*\right)\frac{\psi_1[0]\phi_1[0]^*}{\left(\left|\psi_1[0]\right|^2 + \left|\phi_1[0]\right|^2\right)}, \quad (16)$$

where $\psi_1[0] = \psi_1^{[0]}$, $\phi_1[0] = \phi_1^{[0]}$,

$$H[0] = \begin{pmatrix} \psi_1[0] & -\phi_1[0]^* \\ \phi_1[0] & \psi_1[0]^* \end{pmatrix}, \quad \Lambda_1 = \begin{pmatrix} \zeta_1 & 0 \\ 0 & \zeta_1^* \end{pmatrix}.$$

(2) The second-step generalized DT follows.

In light of the first-step case, we realize that $T[1]\Psi_1$ is a solution to the Lax pair equations (8) and (9)) for $q = q[1]$ and $\zeta = \zeta_1 + \delta$. Therefore, the following limit:

$$\lim_{\delta\to 0}\frac{T[1]\big|_{\zeta=\zeta_1+\delta}\Psi_1}{\delta} = \lim_{\delta\to 0}\frac{(\delta + T_1[1])\Psi_1}{\delta} = \Psi_1^{[0]} + T_1[1]\Psi_1^{[1]} \equiv \Psi_1[1]$$

offers a nontrivial solution to the Lax pair equations (8) and (9) for $q = q[1]$ and $\zeta = \zeta_1$. At this point, the second-step generalized DT holds:

$$\Psi[2] = T[2]T[1]\Psi, \ T[2] = \zeta I - H[1]\Lambda_2 H[1]^{-1}, \quad (17)$$

$$q[2] = q[1] - 2\mathrm{i}\left(\zeta_1 - \zeta_1^*\right)\frac{\psi_1[1]\phi_1[1]^*}{\left(\left|\psi_1[1]\right|^2 + \left|\phi_1[1]\right|^2\right)}, \quad (18)$$

where $(\psi_1[1], \phi_1[1])^T = \Psi_1[1]$,

$$H[1] = \begin{pmatrix} \psi_1[1] & -\phi_1[1]^* \\ \phi_1[1] & \psi_1[1]^* \end{pmatrix}, \quad \Lambda_2 = \begin{pmatrix} \zeta_1 & 0 \\ 0 & \zeta_1^* \end{pmatrix}.$$

(3) The third-step generalized DT follows.

Analogous to the foregoing, we consider the following limit:

$$\lim_{\delta\to 0}\frac{[T[2]T[1]]\big|_{\zeta=\zeta_1+\delta}\Psi_1}{\delta^2} = \lim_{\delta\to 0}\frac{(\delta + T_1[2])(\delta + T_1[1])\Psi_1}{\delta^2}$$
$$= \Psi_1^{[0]} + (T_1[2] + T_1[1])\Psi_1^{[1]} + T_1[2]T_1[1]\Psi_1^{[2]} \equiv \Psi_1[2].$$

Here we have used the identity

$$T_1[1]\Psi_1^{[0]} = 0, \ T_1[2](\Psi_1^{[0]} + T_1[1]\Psi_1^{[1]}) = 0.$$

Hence we obtain a nontrivial solution to the Lax pair equations (8) and (9) for $q = q[2]$ and $\zeta = \zeta_1$. The third-step generalized DT follows:

$$\Psi[3] = T[3]T[2]T[1]\Psi, \ T[3] = \zeta I - H[2]\Lambda_3 H[2]^{-1}, \quad (19)$$

$$q[3] = q[2] - 2\mathrm{i}\left(\zeta_1 - \zeta_1^*\right)\frac{\psi_1[2]\phi_1[2]^*}{\left(\left|\psi_1[2]\right|^2 + \left|\phi_1[2]\right|^2\right)}, \quad (20)$$

where $(\psi_1[2], \phi_1[2])^T = \Psi_1[2]$,

$$H[2] = \begin{pmatrix} \psi_1[2] & -\phi_1[2]^* \\ \phi_1[2] & \psi_1[2]^* \end{pmatrix}, \quad \Lambda_3 = \begin{pmatrix} \zeta_1 & 0 \\ 0 & \zeta_1^* \end{pmatrix}.$$

Continuing the foregoing process and combining all the generalized DTs, the general case can be given.

Proposition 2. *Denoting*

$$\Psi_1[l] = \Psi_1^{[0]} + \sum_{j=1}^{l} T_1[j]\Psi_1^{[1]} + \sum_{j=1}^{l}\sum_{k=1}^{j-1} T_1[j]T_1[k]\Psi_1^{[2]} + \ldots + T_1[l]T_1[l-1]\ldots T_1[1]\Psi_1^{[l]},$$

then the Nth-step generalized DT yields

$$\Psi[N] = T[N]T[N-1]\ldots T[1]\Psi, \ T[l] = \zeta I - H[l-1]\Lambda_l H[l-1]^{-1}, \quad (21)$$

$$q[N] = q[0] - 2\mathrm{i}\left(\zeta_1 - \zeta_1^*\right)\sum_{l=0}^{N-1}\frac{\psi_1[l]\phi_1[l]^*}{\left(\left|\psi_1[l]\right|^2 + \left|\phi_1[l]\right|^2\right)}, \quad (22)$$

where

$$\left(\psi_1[l], \phi_1[l]\right)^T = \Psi_1[l]$$

$$H[l-1] = \begin{pmatrix} \psi_1[l-1] & -\phi_1[l-1]^* \\ \phi_1[l-1] & \psi_1[l-1]^* \end{pmatrix},$$

$$\Lambda_l = \begin{pmatrix} \zeta_1 & 0 \\ 0 & \zeta_1^* \end{pmatrix}, \quad 1 \leqslant l \leqslant N.$$

In what follows, on the basis of the Crum theorem [35] and the determinant representation of the Nth-step generalized DT for the NLS equation [21], we give the $2N \times 2N$ determinant representation of (22).

Proposition 3. *Define*

$$\left(\zeta_1 + \delta\right)^j\psi_1\left(\zeta_1 + \delta\right) = \zeta_1^j\psi_1^{[0]} + \psi_1[j, 1]\delta + \psi_1[j, 2]\delta^2 + \ldots + \psi_1[j, m]\delta^m + \ldots,$$

$$\left(\zeta_1 + \delta\right)^j\phi_1\left(\zeta_1 + \delta\right) = \zeta_1^j\phi_1^{[0]} + \phi_1[j, 1]\delta + \phi_1[j, 2]\delta^2 + \ldots + \phi_1[j, m]\delta^m + \ldots,$$

$(j = 0, 1, \ldots, \ m = 1, 2, \ldots)$, *with*

$$\psi_1[j, m] = \frac{1}{m!}\frac{\partial^m}{\partial\delta^m}\left[\left(\zeta_1 + \delta\right)^j\psi_1\left(\zeta_1 + \delta\right)\right]\Big|_{\delta=0},$$

$$\phi_1[j, m] = \frac{1}{m!}\frac{\partial^m}{\partial\delta^m}\left[\left(\zeta_1 + \delta\right)^j\phi_1\left(\zeta_1 + \delta\right)\right]\Big|_{\delta=0}.$$

Then (22) can be rewritten as

$$q[N] = q[0] - 2\mathrm{i}\frac{|\Omega_1|}{|\Omega|}, \tag{23}$$

where

$$\Omega_1 = \begin{pmatrix} \psi_1^{[0]} & -\phi_1^{[0]*} & \psi_1[0,1] & -\phi_1[0,1]^* & \cdots & \psi_1[0,N-1] & -\phi_1[0,N-1]^* \\ \phi_1^{[0]} & \psi_1^{[0]*} & \phi_1[0,1] & \psi_1[0,1]^* & \cdots & \phi_1[0,N-1] & \psi_1[0,N-1]^* \\ \zeta_1\psi_1^{[0]} & -\zeta_1^*\phi_1^{[0]*} & \psi_1[1,1] & -\phi_1[1,1]^* & \cdots & \psi_1[1,N-1] & -\phi_1[1,N-1]^* \\ \zeta_1\phi_1^{[0]} & \zeta_1^*\psi_1^{[0]*} & \phi_1[1,1] & \psi_1[1,1]^* & \cdots & \phi_1[1,N-1] & \psi_1[1,N-1]^* \\ \cdots & \cdots & \cdots & \cdots & \cdots & \cdots & \cdots \\ \zeta_1^{N-1}\psi_1^{[0]} & -\zeta_1^{*N-1}\phi_1^{[0]*} & \psi_1[N-1,1] & -\phi_1[N-1,1]^* & \cdots & \psi_1[N-1,N-1] & -\phi_1[N-1,N-1]^* \\ \zeta_1^{N}\psi_1^{[0]} & -\zeta_1^{*N}\psi_1^{[0]*} & \psi_1[N,1] & -\psi_1[N,1]^* & \cdots & \psi_1[N,N-1] & -\phi_1[N,N-1]^* \end{pmatrix},$$

and

$$\Omega = \begin{pmatrix} \psi_1^{[0]} & -\phi_1^{[0]*} & \psi_1[0,1] & -\phi_1[0,1]^* & \cdots & \psi_1[0,N-1] & -\phi_1[0,N-1]^* \\ \phi_1^{[0]} & \psi_1^{[0]*} & \phi_1[0,1] & \psi_1[0,1]^* & \cdots & \phi_1[0,N-1] & \psi_1[0,N-1]^* \\ \zeta_1\psi_1^{[0]} & -\zeta_1^*\phi_1^{[0]*} & \psi_1[1,1] & -\phi_1[1,1]^* & \cdots & \psi_1[1,N-1] & -\phi_1[1,N-1]^* \\ \zeta_1\phi_1^{[0]} & \zeta_1^*\psi_1^{[0]*} & \phi_1[1,1] & \psi_1[1,1]^* & \cdots & \phi_1[1,N-1] & \psi_1[1,N-1]^* \\ \cdots & \cdots & \cdots & \cdots & \cdots & \cdots & \cdots \\ \zeta_1^{N-1}\psi_1^{[0]} & -\zeta_1^{*N-1}\phi_1^{[0]*} & \psi_1[N-1,1] & -\phi_1[N-1,1]^* & \cdots & \psi_1[N-1,N-1] & -\phi_1[N-1,N-1]^* \\ \zeta_1^{N-1}\phi_1^{[0]} & \zeta_1^{*N-1}\psi_1^{[0]*} & \phi_1[N-1,1] & \psi_1[N-1,1]^* & \cdots & \phi_1[N-1,N-1] & \psi_1[N-1,N-1]^* \end{pmatrix}.$$

Remark 2. What we should mention is that both (22) and (23) lead to the Nth-order rogue wave solution to equation (3). But in a practical application, we prefer to use the Darboux transformation of degree one successively (22) rather than a Darboux transformation with the high-order determinant representation (23), so as to avoid the cumbersome calculation of the determinant of a matrix with a high order. Because the algorithm of the Darboux transformation of degree one is purely algebraic and independent of the seed solution, it is convenient for working out the solutions by using symbolic computation via computer.

At this point, we arrive at a simple unified formula for an Nth-order rogue wave solution for equation (2).

Proposition 4. *Let $q[N]$ defined by (22) be a solution to the extended NLS equation (3); then the following formula:*

$$u[N] = q[N]\exp\left(2\mathrm{i}\beta\int\left|q[N]\right|^2 dx\right) \tag{24}$$

provides the explicit Nth-order rogue wave solution to the KE equation.

Here it is shown that we only have to work out rogue wave solutions to equation (3); then the formula (24) gives rise to the corresponding arbitrary-order rogue wave solutions to equation (2). In the next section, we present some explicit rogue wave solutions to equation (2) to illustrate how to use the preceding formula.

4. Rogue wave solutions

In this section, we start from a nontrivial seed solution to equation (2),

$$u[0] = \alpha\exp\left[\mathrm{i}\theta_1\right],$$
$$\theta_1 = ax + \left(-a^2 + 2\alpha^2 + 4\beta^2\alpha^4\right)t, \tag{25}$$

where α, a are real parameters. Without losing generality, we set $\alpha = 1$, $a = 0$; then (25) is reduced to $u[0] = \exp\left[\mathrm{i}(4\beta^2 + 2)t\right]$. From the gauge transformation between equations (2) and (3), a nontrivial seed solution to equation (3) can be obtained as

$$q[0] = \exp\left[\mathrm{i}\theta\right],\quad \theta = -2\beta x + \left(4\beta^2 + 2\right)t. \tag{26}$$

According to the preceding section, we know that it is essential to obtain a basic solution to the Lax pair equations (8) and (9) that can be expanded as a Taylor series. To this end, motivated by the work of using DT theory [21, 53, 54], we take $\zeta = \beta + \mathrm{i}h$, and then, solving the Lax pair equations under the nontrivial seed solution (26) and this

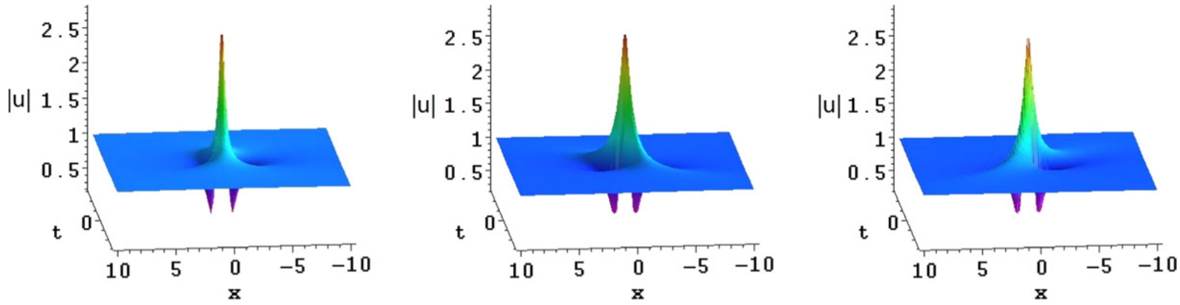

(a) (b) (c)

Figure 1. Evolution plot of the first-order rogue wave solution (29): (a) $\beta = 0$; (b) $\beta = 1/3$; (c) $\beta = -1/3$.

special spectral parameter, we obtain

$$\Psi_1 = \begin{pmatrix} \left(C_1 e^{\eta} - C_2 e^{-\eta}\right) e^{\frac{i}{2}\theta} \\ \left(C_1 e^{-\eta} - C_2 e^{\eta}\right) e^{-\frac{i}{2}\theta} \end{pmatrix}, \tag{27}$$

where

$$C_1 = \frac{\left(h - \sqrt{h^2 - 1}\right)^{\frac{1}{2}}}{\sqrt{h^2 - 1}}, \quad C_2 = \frac{\left(h + \sqrt{h^2 - 1}\right)^{\frac{1}{2}}}{\sqrt{h^2 - 1}},$$

$$\eta = -\sqrt{h^2 - 1}\left(x + 4\beta t + 2iht + \sum_{k=1}^{N} s_k f^{2k}\right),$$

where $s_k = m_k + in_k$, $(m_k, n_k \in \mathbb{R})$ and f is a small parameter.

Taking $h = 1 - if^2$, the vector function $\Psi_1(f)$ can be expanded as a Taylor series at f=0, that is,

$$\Psi_1(f) = \Psi_1^{[0]} + \Psi_1^{[1]} f^2 + \Psi_1^{[2]} f^4 + \ldots, \tag{28}$$

where $\Psi_1^{[j]} = \left(\psi_1^{[j]}, \phi_1^{[j]}\right)^T$, $(j = 0, 1, 2)$ are explicitly given in appendix A.

It is straightforward to verify that $\Psi_1^{[0]}$ is a solution to the Lax pair equations (8) and (9) for $q = q[0]$ and $\zeta = \zeta_1 = \beta + i$. In the following, by virtue of the formula (22) with N=1, we calculate that

$$q[1] = \exp[i\theta] \frac{F_1 + iG_1}{D_1},$$

where

$$F_1 = -4x^2 - 32\beta tx - 16\left(4\beta^2 + 1\right)t^2 + 3, \quad G_1 = 16t,$$
$$D_1 = 4x^2 + 32\beta tx + 16\left(4\beta^2 + 1\right)t^2 + 1.$$

Afterwards, the explicit first-order rogue wave solution to equation (2) can be obtained as

$$u[1] = q[1] \exp\left[2i\beta \int \left|q[1]\right|^2 dx\right], \tag{29}$$

where, $\int |q[1]|^2 dx = \frac{H_1}{D_1}$ with

$$H_1 = 4x^3 + 16\left(4\beta^2 + 1\right)t^2 x + 9x + 32\beta\left(x^2 + 1\right)t.$$

It is easy to verify the validity of the solution by putting it back into equation (2), and we see that there is a free parameter β in the preceding solution. Now we discuss the dynamic properties of the preceding solution. When $\beta = 0$, (29) is just the standard Peregrine soliton solution to the NLS equation [16]; see figures 1(a) and 2(a). There are one hump and two valleys around the center: the maximum value of the hump is 3 and occurs at (0,0), and the minimum value of the two valleys is 0 and occurs at (±0.8660, 0). When $\beta \neq 0$, we see that the shape of the rogue wave does not change drastically; see figures 1(b) and 1(c). However, the quintic andRaman-effect nonlinear terms do produce an important skew angle relative to the ridge of the rogue wave in the counter clockwise direction if $\beta > 0$, and in the clockwise direction if $\beta < 0$; see figures 2(b) and (d). Moreover, as the absolute value of β gets larger, the skew angle becomes larger; see figures 2(b)–(e).

Next, the following limit,

$$\lim_{f \to 0} \frac{T[1]\big|_{\zeta = \beta + i + f^2} \Psi_1}{f^2} = \lim_{f \to 0} \frac{\left(f^2 + T_1[1]\right)\Psi_1}{f^2}$$
$$= \Psi_1^{[0]} + T_1[1]\Psi_1^{[1]} \equiv \Psi_1[1],$$

provides the generating function of the second-step generalized DT. Hence, resorting to the formula (22) with $N = 2$, we have

$$q[2] = \exp[i\theta] \frac{F_2 + iG_2}{D_2},$$

where

$$\begin{aligned} F_2 = {} & 64x^6 - 144x^4 + 192n_1x^3 - 180x^2 \\ & + 24576\beta\left(4\beta^2 + 1\right)^2 t^5 x + 432n_1 x \\ & + 4096\left(4\beta^2 + 1\right)^3 t^6 + \Big(3072\left(20\beta^2 + 1\right)\left(4\beta^2 + 1\right)x^2 \\ & - 36864\beta^4 - 92160\beta^2 - 8448\Big)t^4 \\ & + \Big(4096\beta\left(20\beta^2 + 3\right)x^3 - 9216\beta\left(4\beta^2 + 5\right)x \\ & + 1536m_1 - 18432\beta^2 m_1 - 9216\beta n_1 + 12288\beta^3 n_1\Big)t^3 \\ & + \Big(\left(15360\beta^2 + 768\right)x^4 - \left(13824\beta^2 + 5760\right)x^2 \end{aligned}$$

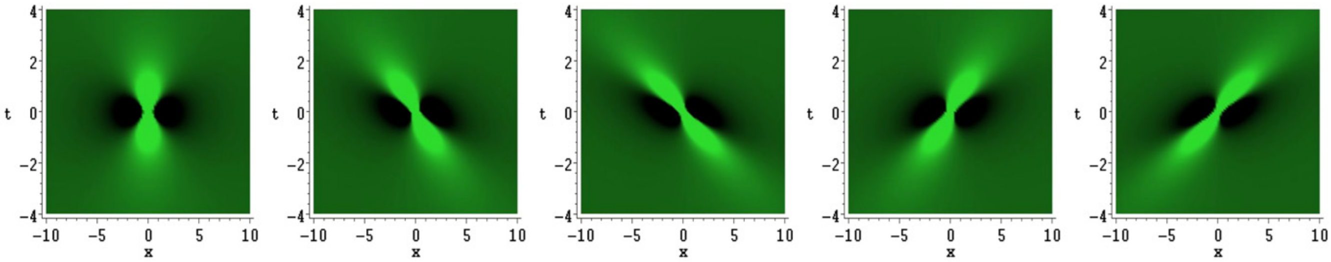

(a) (b) (c) (d) (e)

Figure 2. Evolution density plot of the first-order rogue wave solution (29): (a) $\beta = 0$; (b) $\beta = 1/3$; (c) $\beta = 1/2$; (d) $\beta = -1/3$; (e) $\beta = -1/2$.

$$
\begin{aligned}
&-\left(9216\beta m_1 - 9216\beta^2 n_1 + 2304 n_1\right)x - 2880\beta^2 \\
&-1872)\, t^2 + (1536\,\beta x^5 - 2304\beta x^3 - \left(1152 m_1 \right.\\
&\left.-2304\beta n_1\right)x^2 - 1440\beta x \\
&-288 m_1 + 1728\beta n_1)\, t + 45 + 144 m_1^2 + 144 n_1^2,
\end{aligned}
$$

$$
\begin{aligned}
G_2 = {} & 576 m_1 x^2 - 49152\beta\left(4\beta^2 + 1\right)t^4 x - 12288\left(4\beta^2 + 1\right)^2 t^5 \\
&-\left(\left(73728\beta^2 + 6144\right)x^2 - 18432\beta^2 + 1536\right)t^3 \\
&-\left(12288\beta x^3 - 9216\beta x - 9216\beta^2 m_1 + 2304 m_1 \right.\\
&\left.-9216\beta n_1\right)t^2 - \left(768 x^4 - 1152 x^2 \right.\\
&\left.-(4608\beta m_1 + 2304 n_1)x - 720\right)t + 144 m_1,
\end{aligned}
$$

$$
\begin{aligned}
D_2 = {} & 64x^6 + 48x^4 + 192 n_1 x^3 + 108 x^2 \\
&+24576\beta\left(4\beta^2 + 1\right)^2 t^5 x - 144 n_1 x \\
&+4096\left(4\beta^2 + 1\right)^3 t^6 + \left(3072\left(20\beta^2 + 1\right)\right.\\
&\left.\times\left(4\beta^2 + 1\right)x^2 + 768\left(4\beta^2 - 3\right)^2\right)t^4 \\
&+\left(4096\beta\left(20\beta^2 + 3\right)x^3\right.\\
&+3072\beta\left(4\beta^2 - 3\right)x + 1536 m_1 - 18432\beta^2 m_1 \\
&\left.-9216\beta n_1 + 12288\beta^3 n_1\right)t^3 \\
&+\left(\left(15360\beta^2 + 768\right)x^4 + 1152(2\beta - 1)(2\beta + 1)x^2\right.\\
&-\left(9216\beta m_1 + 2304 n_1 - 9216\beta^2 n_1\right)x \\
&\left.+1728\beta^2 + 1584\right)t^2 \\
&+\left(1536\beta x^5 + 768\beta x^3 - \left(1152 m_1 - 2304 n_1\beta\right)x^2\right.\\
&\left.+864\beta x + 864 m_1 - 576 n_1\beta\right)t \\
&+144 m_1^2 + 144 n_1^2 + 9.
\end{aligned}
$$

After that, the explicit second-order rogue wave solution to equation (2) takes the form of

$$
u[2] = q[2]\exp\left[2\mathrm{i}\beta\int\left|q[2]\right|^2 dx\right], \tag{30}
$$

where $\int |q[2]|^2 dx = \frac{H_2}{D_2}$ with

$$
\begin{aligned}
H_2 = {} & 64x^7 + 432x^5 + 192 n_1 x^4 + 300 x^3 \\
&+432 n_1 x^2 + 4096\left(4\beta^2 + 1\right)^3 t^6 x \\
&+\left(144 m_1^2 + 144 n_1^2 + 225\right)x \\
&+\left(24576\beta \times \left(4\beta^2 + 1\right)^2 x^2\right.\\
&\left.+24576\beta\left(4\beta^2 + 1\right)^2\right)t^5 \\
&+\left(3072\left(20\beta^2 + 1\right)\left(4\beta^2 + 1\right)x^3\right.\\
&\left.+\left(503808\beta^4 + 129024\beta^2 + 13056\right)x\right)t^4 \\
&+\left(4096\beta\left(20\beta^2 + 3\right)x^4 + 9216\beta\left(28\beta^2 + 3\right)x^2\right.\\
&+\left(1536 m_1 - 18432\beta^2 m_1 - 9216\beta n_1 + 12288\beta^3 n_1\right)x \\
&\left.+3072\beta\left(4\beta^2 - 3\right)\right)t^3 \\
&+\left(\left(15360\beta^2 + 768\right)x^5 + \left(66048\beta^2 + 1920\right)x^3\right.\\
&-\left(9216\beta m_1 + 2304 n_1 - 9216\beta^2 n_1\right)x^2 \\
&+\left(10944\beta^2 - 720\right)x - 9216\beta m_1 \\
&\left.-2304 n_1 + 9216\beta^2 n_1\right)t^2 + \left(1536\beta x^6\right.\\
&+8448\beta x^4 - \left(1152 m_1 - 2304 n_1\beta\right)x^3 + 3168\beta x^2 \\
&\left.-\left(1440 m_1 - 4032 n_1\beta\right)x + 864\beta\right)t - 144 n_1.
\end{aligned}
$$

It is straightforward to check, with the aid of Maple, that the preceding solution satisfies equation (2).

By setting $m_1 = 0$, $n_1 = 0$ in the preceding solution, we obtain the fundamental second-order rogue wave solution to equation (2). In this case, it is easy to compute that $x \to \infty$, $t \to \infty$, $|u[2]| \to 1$ and that the maximum value 5 arrives at (0, 0). In addition, similar to the first-order case, the quintic and Raman-effect nonlinear terms also produce a skew angle relative to the ridge of the rogue wave; see figure 3.

Apart from this, by setting $m_1 = 100$, $n_1 = 0$, the fundamental second-order rogue wave can be separated into three first-order rogue waves: a single and a double spatial hump; see figure 4. If $\beta = 0$, we observe that in figure 4(a), a single hump appears at $t \approx -2.5626$ and then swiftly decays, with

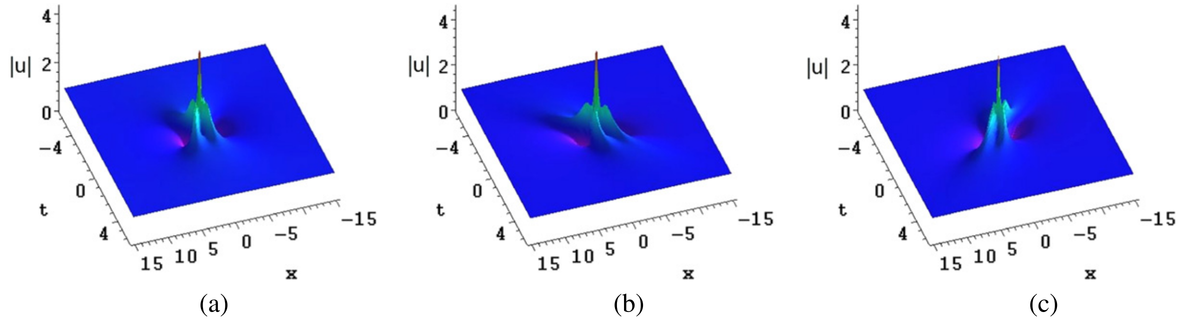

Figure 3. Evolution plot of the second-order rogue wave solution (30) with $m_1 = 0,\ n_1 = 0$: (a) $\beta = 0$; (b) $\beta = 1/3$; (c) $\beta = -1/3$.

two spatial humps rising up simultaneously at $t \approx 1.3169$, and the corresponding spatial coordinates are $x = 0$, $x \approx \pm\, 4.6411$, respectively. If $\beta > 0$, for example, $\beta = 1/3$, we see that in figure 4(b), a single hump and two spatial humps successively rise and climb to the maximum amplitude at $t \approx -2.5626$ and $t \approx 1.3169$, which is identical to the case of $\beta = 0$. Nevertheless, the single hump has a translation in the positive direction of the x-axis and its spatial coordinate becomes $x \approx 3.4168$, whereas the double spatial hump moves in the negative direction of the x-axis and the spatial coordinates change to $x \approx 2.8853$ and $x \approx -6.3970$. The detailed variation and spatial-temporal coordinates of maximum amplitudes of the second-order rogue wave with triangular pattern are listed in table 1. From figure 4(c) and table 1, we notice that as β gets larger, the amplitudes and the time of appearance of the humps remain unchanged, but the humps have a larger movement in the direction of the x-axis. If $\beta < 0$, the humps will have translations in the opposite direction of the x-axis and, comparing with the case of $\beta > 0$, the amplitudes and the time of appearance of the humps are still unchanged; see figures 4(d)–(e) and table 1.

Similarly, the following limit,

$$\lim_{f\to 0}\frac{[T[2]T[1]]\big|_{\zeta=\beta+\mathrm{i}+f^2}\Psi_1}{f^4} = \lim_{f\to 0}\frac{(f^2+T_1[2])(f^2+T_1[1])\Psi_1}{f^4}$$
$$=\Psi_1^{[0]} + \left(T_1[2]+T_1[1]\right)\Psi_1^{[1]} + T_1[2]T_1[1]\Psi_1^{[2]} \equiv \Psi_1[2],$$

is the generating function of the third-order generalized DT. With the aid of (22) and (24), the third-order rogue wave solution to equation (2) can be obtained. Here we give only the explicit expression of the fundamental third-order rogue wave solution (see appendix B). The parameters are chosen as $m_1 = 0,\ n_1 = 0,\ m_2 = 0,\ n_2 = 0$.

From the concrete expressions given in appendix B, we can work out that the maximum value of $|u[3]|$ is 7 and is reached at (0,0). Moreover, the quintic and Raman-effect nonlinear terms still produce a skew angle relative to the ridge of the third-order rogue wave; see figure 5.

In choosing $m_1 = 100,\ n_1 = 0,\ m_2 = 0,\ n_2 = 0$, the fundamental third-order rogue wave splits into six first-order rogue waves forming a triangle; see figure 6. In figure 6(a), as $\beta = 0$, we see that a single hump develops at $t \approx -4.5319$, and then two rogue waves symmetrically appear at $t \approx -1.2237$. Finally, a triple spatial hump soon rises up at $t \approx 2.3807$ and $t \approx 2.5135$. In figure 6(b), as $\beta = 1/3$, we observe that the time for the appearance of the humps is invariable, the single hump and the double spatial hump have translations in the positive direction of the x-axis, and the triple spatial hump has a translation in the negative direction of the x-axis. Table 2 is presented to show the detailed variation and spatial-temporal coordinates of maximum amplitudes in the third-order rogue wave with triangular pattern. As with the second-order case, we see that in figure 6(c) and table 2, as β gets larger, a larger movement for the humps in the direction of the x-axis is produced by the the quintic and Raman-effect nonlinear terms, whereas the amplitudes and the time of appearance of the humps remain unchanged. In addition, comparing with the case where $\beta > 0$, as $\beta < 0$, the humps will have a movement in the opposite direction of the x-axis; see figures 6(d)–(e) and table 2. Here it should be mentioned that although some errors and disparities indeed exist in the calculation of the maximum amplitudes and the spatial-temporal coordinates of the humps in rogue waves, the main dynamic properties of the rogue waves and the influences produced by the nonlinear terms on the rogue waves remain the same. Furthermore, when letting $m_1 = 0$, $n_1 = 0,\ m_2 = 10000,\ n_2 = 0$, the third-order rogue wave of circular pattern can be presented, and the quintic and Raman-effect nonlinear terms can also produce a translation for the humps in the direction of the x-axis; see figure 7.

Next, continuing the iterative process, the fourth-order rogue wave solution to equation (2) can be obtained. Here, we omit the cumbersome expression and just show some particular figures; see figure 8. The fundamental pattern is shown in figure 8(a). We see that a single highest peak is localized in the center and its amplitude is 9, and because of the existence of the quintic and Raman-effect nonlinear terms, there is a skew angle relative to the ridge of the rogue wave. The triangular pattern with one, two, three, and four peaks successively arrayed in each temporal row is displayed in figure 8(b); and the pentagram pattern, shown in figure 8(c), contains two concentric circles, each with five humps. Figure 8(d) describes the heptagram pattern, which is composed of seven Peregrine solitons in the outer ring and a second-order rogue wave in the center. By adequately adjusting the free parameters, the middle second-order rogue wave can split into three Peregrine solitons; see figure 8(e).

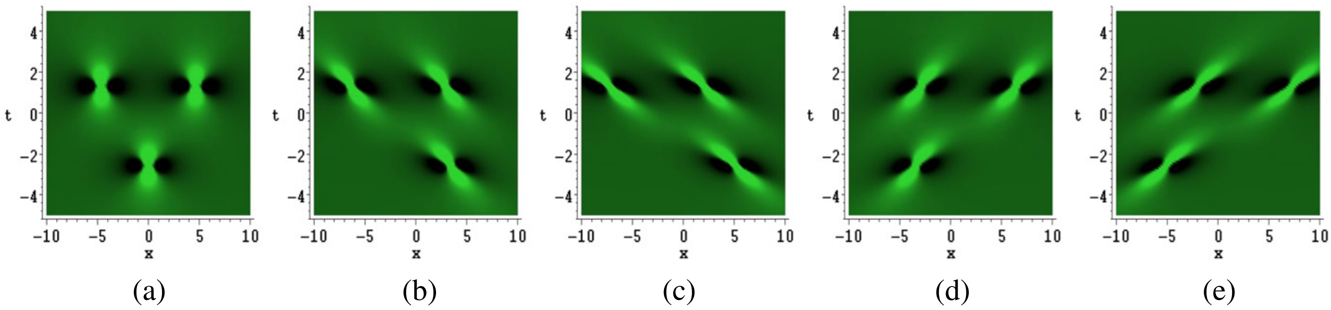

Figure 4. Evolution density plot of the second-order rogue wave solution (30) with $m_1 = 100$, $n_1 = 0$: (a) $\beta = 0$; (b) $\beta = 1/3$; (c) $\beta = 1/2$; (d) $\beta = -1/3$; (e) $\beta = -1/2$.

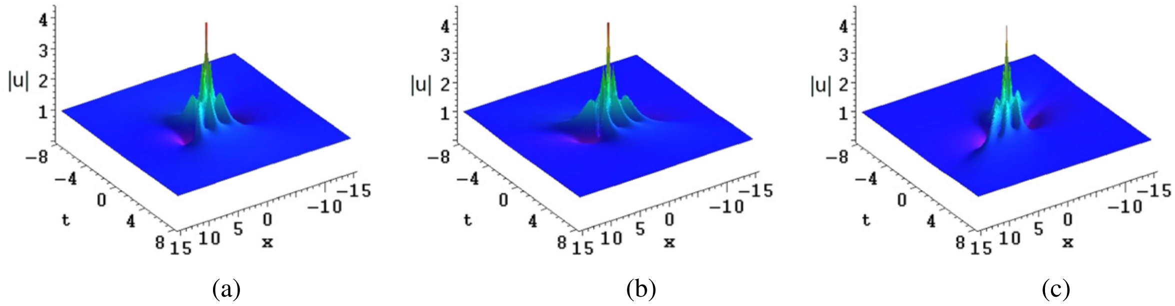

Figure 5. Evolution plot of the third-order rogue wave solution with $m_1 = 0$, $n_1 = 0$, $m_2 = 0$, $n_2 = 0$: (a) $\beta = 0$; (b) $\beta = 1/3$; (c) $\beta = -1/3$.

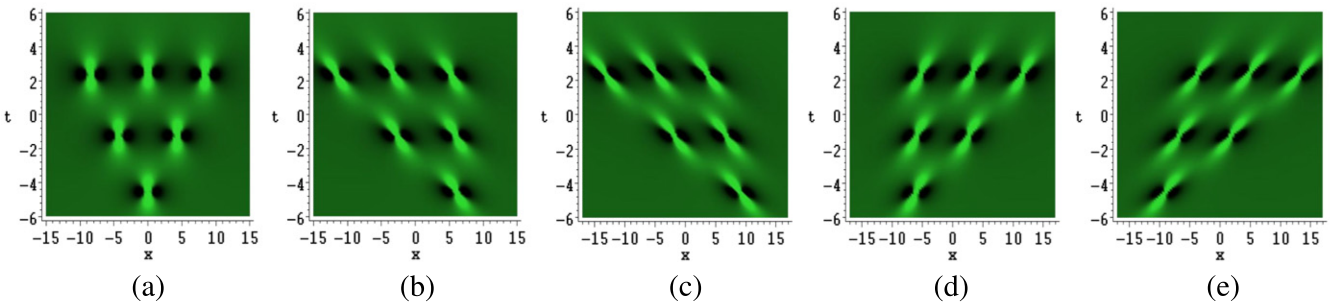

Figure 6. Evolution density plot of the third-order rogue wave solution with $m_1 = 100$, $n_1 = 0$, $m_2 = 0$, $n_2 = 0$: (a) $\beta = 0$; (b) $\beta = 1/3$; (c) $\beta = 1/2$; (d) $\beta = -1/3$; (e) $\beta = -1/2$.

Table 1. Maximum value $|u|^2$ of the humps in the second-order rogue wave with triangular pattern

β	Single spatial hump	Double spatial hump
0	$9.2235(x = 0,\ t = -2.5626)$	$8.8950(x = -4.6411,\ t = 1.3169)$, $8.8950(x = 4.6411,\ t = 1.3169)$
1/3	$9.2235(x = 3.4168,\ t = -2.5626)$	$8.8950(x = -6.3970,\ t = 1.3169)$, $8.8950(x = 2.8853,\ t = 1.3169)$
1/2	$9.2235(x = 5.1252,\ t = -2.5626)$	$8.8950(x = -7.2749,\ t = 1.3169)$, $8.8950(x = 2.0074,\ t = 1.3169)$
-1/3	$9.2235(x = -3.4168,\ t = -2.5626)$	$8.8950(x = -2.8853,\ t = 1.3169)$, $8.8950(x = 6.3970,\ t = 1.3169)$
-1/2	$9.2235(x = -5.1252,\ t = -2.5626)$	$8.8950(x = -2.0074,\ t = 1.3169)$, $8.8950(x = 7.2749,\ t = 1.3169)$

5. Conclusion

In summary, we studied higher-order rogue wave solutions of the KE equation, which contains quintic nonlinearity and Raman effect in nonlinear optics. By means of a gauge transformation, the KE equation was transformed into an extended NLS equation (3) whose Lax pair is the standard AKNS spectral problem and the corresponding auxiliary spectral problem.

Based on a special solution (27) of the Lax pair equations (8) and (9) for $q = q[0]$ and $\zeta = \beta + ih$, a generalized DT and an Nth-order rogue wave solution to the extended NLS equation (3) were constructed by using the limiting technique. Hence, by resorting to the gauge

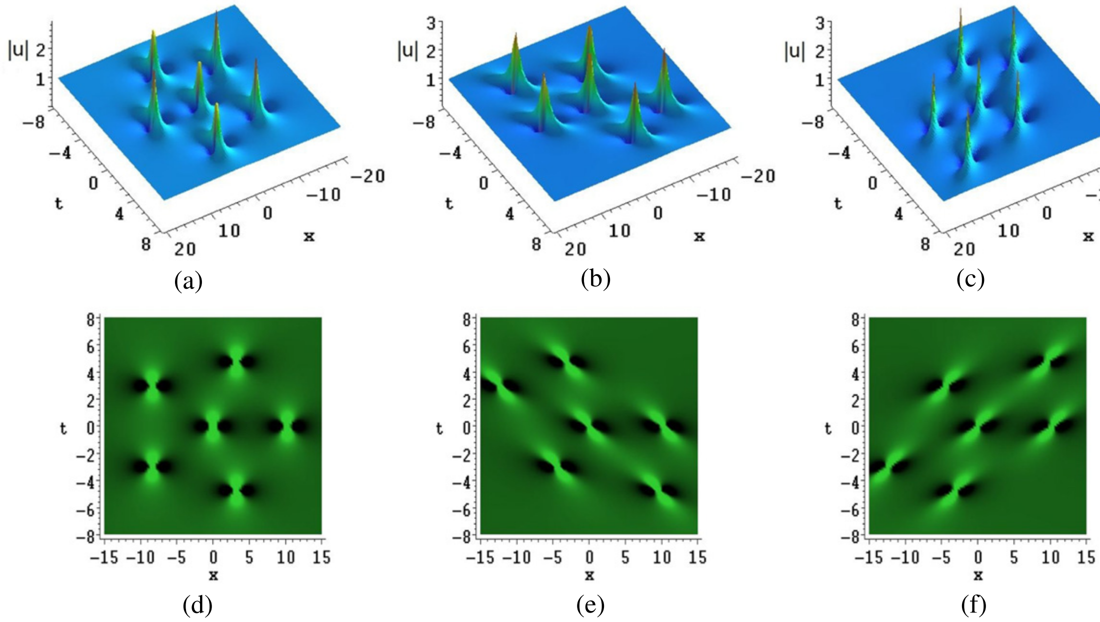

Figure 7. Evolution plot of the third-order rogue wave solution with $m_1 = 0$, $n_1 = 0$, $m_2 = 10000$, $n_2 = 0$: (a), (d) $\beta = 0$; (b), (e) $\beta = 1/3$; (c), (f) $\beta = -1/3$.

Table 2. Maximum value $|u|^2$ of the humps in the third-order rogue wave with triangular pattern

β	Single spatial hump	Double spatial hump
0	$9.4178(x = 0, t = -4.5319)$	$9.1035(x = -4.2981, t = -1.2237)$, $9.1035(x = 4.2981, t = -1.2237)$
1/3	$9.4178(x = 6.0425, t = -4.5319)$	$9.1035(x = -2.6666, t = -1.2237)$, $9.1035(x = 5.9297, t = -1.2237)$
1/2	$9.4178(x = 9.0636, t = -4.5319)$	$9.1035(x = -1.8508, t = -1.2237)$, $9.1035(x = 6.7455, t = -1.2237)$
−1/3	$9.4178(x = -6.0425, t = -4.5319)$	$9.1035(x = -5.9297, t = -1.2237)$, $9.1035(x = 2.6666, t = -1.2237)$
−1/2	$9.4178(x = -9.0636, t = -4.5319)$	$9.1035(x = -6.7455, t = -1.2237)$, $9.1035(x = 1.8508, t = -1.2237)$
	Triple spatial hump	
$8.8132(x = -8.4380, t = 2.3807)$,	$8.8047(x = 0, t = 2.5135)$,	$8.8132(x = 8.4380, t = 2.3807)$
$8.8132(x = -11.6122, t = 2.3807)$,	$8.8047(x = -3.3513, t = 2.5135)$,	$8.8132(x = 5.2638, t = 2.3807)$
$8.8132(x = -13.1993, t = 2.3807)$,	$8.8047(x = -5.0269, t = 2.5135)$,	$8.8132(x = 3.6767, t = 2.3807)$
$8.8132(x = -5.2638, t = 2.3807)$,	$8.8047(x = 3.3513, t = 2.5135)$,	$8.8132(x = 11.6122, t = 2.3807)$
$8.8132(x = -3.6767, t = 2.3807)$,	$8.8047(x = 5.0269, t = 2.5135)$,	$8.8132(x = 13.1993, t = 2.3807)$

transformation between the KE equation and the extended NLS equation (3), a concise unified formula for the Nth-order rogue wave solution with several free parameters for the KE equation was derived. Our formula overcomes the difficulty remarked in [37], that is, that one has to solve two complicated partial differential equations to explicitly determine α_j ($j = 1, 2, \ldots$) in each iterative process. Based on symbolic computation, the formula can be used as is to generate higher-order rogue wave solutions to the KE equation. In particular, we presented explicit rogue wave solutions from the first to the third order of the KE equation, and we used figures to illustrate the dynamic properties of the rogue waves from the first to the fourth order. Moreover, by numerical calculations and plots, the influences produced by the quintic and Raman-effect nonlinear terms on the higher-order rogue waves were discussed. It was shown that the quintic and Raman-effect nonlinear terms affect the spatial distribution of the humps in higher-order rogue waves, whereas the amplitudes and the time of appearance of the humps are unchanged.

In addition, rogue waves on spatially periodic background envelopes such as cnoidal waves were recently observed in the NLS equation [55], and it is entirely possible that similar phenomena will be discovered in the KE equation. At the same time, based on the explicit rogue wave solutions to the KE equation given in this paper, the connection between modulation instability and rogue waves may

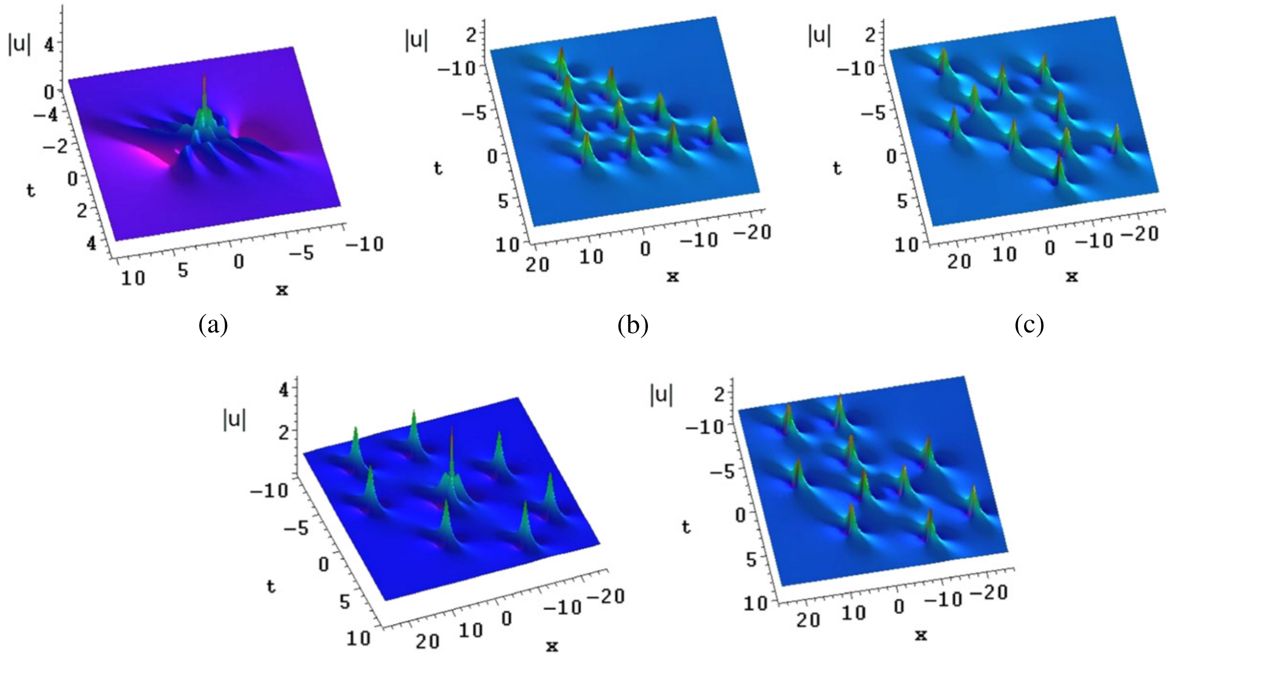

(a) (b) (c) (d) (e)

Figure 8. Evolution plot of the fourth-order rogue wave solution with $\beta = 1/3$: (a) $m_1 = 0$, $n_1 = 0$, $m_2 = 0$, $n_2 = 0$, $m_3 = 0$, $n_3 = 0$; (b) $m_1 = 100$, $n_1 = 0$, $m_2 = 0$, $n_2 = 0$, $m_3 = 0$, $n_3 = 0$; (c) $m_1 = 0$, $n_1 = 0$, $m_2 = 10000$, $n_2 = 0$, $m_3 = 0$, $n_3 = 0$; (d) $m_1 = 0$, $n_1 = 0$, $m_2 = 0$, $n_2 = 0$, $m_3 = 1000000$, $n_3 = 0$; (e) $m_1 = 100$, $n_1 = 0$, $m_2 = 0$, $n_2 = 0$, $m_3 = 1000000$, $n_3 = 0$.

be established for the KE equation by virtue of the method presented in [56], which is instructive for examining the occurrence (or rather the growth phase) of rogue waves. Both problems are important, and we will investigate them in a future paper. Our results will be helpful for better observing the evolution of rogue waves in a complicated optical system with high-order nonlinear terms, and for better understanding the influence produced by the quintic and Raman-effect nonlinear terms on rogue waves. We hope that the results can be verified in real physical experiments in the future.

Acknowledgments

The authors are greatly indebted to the reviewer for helpful comments and constructive suggestions. The project is supported by the National Natural Science Foundation of China (Grant No. 11275072), the Research Fund for the Doctoral Program of Higher Education of China (No. 20120076110024), the Innovative Research Team Program of the National Natural Science Foundation of China (Grant No. 61321064), the Shanghai Knowledge Service Platform for Trustworthy Internet of Things under Grant No. ZF1213, Shanghai Minhang District talents of high level scientific research project, Talent Fund and KC Wong Magna Fund in Ningbo University, National Natural Science Foundation of China (Grant No. 11326165)), and Zhejiang Provincial Natural Science Foundation of China (Grant No. LQ12A01008).

Appendix A. Explicit expressions of coefficients in (27)

$$\psi_1^{[0]} = -\mathrm{e}^{\frac{\mathrm{i}}{2}\theta}(2x - 4\mathrm{i}\tau t + 1),\ \phi_1^{[0]} = \mathrm{e}^{-\frac{\mathrm{i}}{2}\theta}(2x - 4\mathrm{i}\tau t - 1),$$

$$\begin{aligned}\psi_1^{[1]} = &\left(\frac{1}{24} + \frac{\mathrm{i}}{24}\right)\mathrm{e}^{\frac{\mathrm{i}}{2}\theta}(1 - \mathrm{i})\Big(8\mathrm{i}x^3 + 12\mathrm{i}x^2 + 6\mathrm{i}x - 64\tau^3t^3\\ &-\left(96\mathrm{i}\tau^2x + 48\mathrm{i}\tau^2\right)t^2 + \Big(48\tau x^2 + 48\tau x\\ &-12(5 - 2\mathrm{i}\beta)\Big)t - 3\mathrm{i} - 24m_1 - 24\mathrm{i}n_1\Big),\end{aligned}$$

$$\begin{aligned}\phi_1^{[1]} = &-\left(\frac{1}{24} + \frac{\mathrm{i}}{24}\right)\mathrm{e}^{-\frac{\mathrm{i}}{2}\theta}(1 - \mathrm{i})\Big(8\mathrm{i}x^3 - 12\mathrm{i}x^2 + 6\mathrm{i}x\\ &-64\tau^3t^3 - \left(96\mathrm{i}\tau^2x - 48\mathrm{i}\tau^2\right)t^2\\ &+\left(48\tau x^2 - 48\tau x - 12(5 - 2\mathrm{i}\beta)\right)t\\ &+3\mathrm{i} - 24m_1 - 24\mathrm{i}n_1\Big),\end{aligned}$$

$$\begin{aligned}\psi_1^{[2]} = &-\left(\frac{1}{960} + \frac{\mathrm{i}}{960}\right)\mathrm{e}^{\frac{\mathrm{i}}{2}\theta}(1 + \mathrm{i})\Big(32\mathrm{i}x^5 + 80\mathrm{i}x^4 + 240\mathrm{i}x^3\\ &-120\left(-\mathrm{i} + 8m_1 + 8\mathrm{i}n_1\right)x^2 - 30\left(\mathrm{i} + 32m_1 + 32\mathrm{i}n_1\right)x\\ &+1024\tau^5t^5 + \left(2560\mathrm{i}\tau^4x + 1280\mathrm{i}\tau^4\right)t^4\\ &-\left(2560\tau^3x^2 + 2560\tau^3x + 1920(-5 + 2\mathrm{i}\beta)\tau^2\right)t^3\\ &+\Big(-1280\mathrm{i}\tau^2x^3 - 1920\mathrm{i}\tau^2x^2 + 960\mathrm{i}\tau(11 - 6\mathrm{i}\beta)x\\ &+480\left(9\mathrm{i} + 2\beta - 8m_1 + 16\mathrm{i}m_1\beta - 8\mathrm{i}n_1 - 16\beta n_1\right)\tau\Big)t^2\\ &+\Big(320\tau x^4 + 640\tau x^3 - 480(7 - 6\mathrm{i}\beta)x^2\end{aligned}$$

$$
\begin{aligned}
&+480\mathrm{i}\big(5\mathrm{i}+2\beta-8m_1+16\mathrm{i}\beta m_1-8\mathrm{i}n_1-16\beta n_1\big)x\\
&+60\mathrm{i}\big(7\mathrm{i}-2\beta-32m_1+64\mathrm{i}\beta m_1-32\mathrm{i}n_1-64\beta n_1\big)\Big)t\\
&+45\mathrm{i}-240m_1-240\mathrm{i}n_1-960\mathrm{i}m_2+960n_2\big),
\end{aligned}
$$

$$
\begin{aligned}
\phi_1^{[2]}=&\left(\frac{1}{960}+\frac{\mathrm{i}}{960}\right)\mathrm{e}^{-\frac{\mathrm{i}}{2}\theta}(1+\mathrm{i})\Big(32\mathrm{i}x^5-80\mathrm{i}x^4+240\mathrm{i}x^3\\
&-120\big(\mathrm{i}+8m_1+8\mathrm{i}n_1\big)x^2-30\big(\mathrm{i}-32m_1-32\mathrm{i}n_1\big)x\\
&+1024\tau^5t^5+\Big(2560\mathrm{i}\tau^4x-1280\mathrm{i}\tau^4\Big)t^4\\
&-\Big(2560\tau^3x^2-2560\tau^3x+1920(-5+2\mathrm{i}\beta)\tau^2\Big)t^3\\
&+\Big(-1280\mathrm{i}\tau^2x^3+1920\mathrm{i}\tau^2x^2+960\mathrm{i}\tau(11-6\mathrm{i}\beta)x\\
&+480\big(-9\mathrm{i}-2\beta-8m_1+16\mathrm{i}m_1\beta-8\mathrm{i}n_1-16\beta n_1\big)\tau\Big)t^2\\
&+\Big(320\tau x^4-640\tau x^3-480(7-6\mathrm{i}\beta)x^2\\
&+480\mathrm{i}\big(-5\mathrm{i}-2\beta-8m_1+16\mathrm{i}\beta m_1-8\mathrm{i}n_1-16\beta n_1\big)x\\
&-60\mathrm{i}\big(-7\mathrm{i}+2\beta-32m_1+64\mathrm{i}\beta m_1-32\mathrm{i}n_1-64\beta n_1\big)\Big)t\\
&-45\mathrm{i}-240m_1-240\mathrm{i}n_1-960\mathrm{i}m_2+960n_2\Big),
\end{aligned}
$$

here $\tau=-1+2\mathrm{i}\beta$.

Appendix B. Explicit expressions of *q* [3] and *u* [3]

$$
q[3]=\exp[\mathrm{i}\theta]\frac{F_3+\mathrm{i}G_3}{D_3},
$$

$$
\begin{aligned}
F_3=&-4096x^{12}+18432x^{10}+57600x^8\\
&+172800x^6-226800x^4-113400x^2\\
&-201326592\beta\left(4\beta^2+1\right)^5t^{11}x-16777216\left(4\beta^2+1\right)^6t^{12}\\
&-\Big(25165824\left(44\beta^2+1\right)\left(4\beta^2+1\right)^4x^2\\
&-6291456(48\beta^4+264\beta^2+23)(4\beta^2+1)^3)t^{10}\\
&-(83886080\beta(44\beta^2+3)(4\beta^2+1)^3x^3\\
&-188743680\beta\left(16\beta^4+72\beta^2+9\right)\\
&\times\left(4\beta^2+1\right)^2x\Big)t^9\\
&+\Big(-15728640\left(528\beta^4+72\beta^2+1\right)\\
&\times\left(4\beta^2+1\right)^2x^4\\
&+23592960\left(4\beta^2+1\right)\Big(576\beta^6\\
&+2096\beta^4+396\beta^2+9)x^2+3774873600\beta^8\\
&-8304721920\beta^6-2359296000\beta^4-896532480\beta^2\\
&+533790720)t^8+(-25165824\beta(4\beta^2+1)\\
&\times\Big(528\beta^4+120\beta^2+5\Big)x^5\\
&+62914560\beta\left(12\beta^2+1\right)\Big(48\beta^4+136\beta^2+27\Big)x^3\\
&\times23592960\beta\Big(320\beta^6-528\beta^4-100\beta^2-19\Big)x\Big)t^7\\
&+(-(15502147584\beta^6+5284823040\beta^4\\
&+440401920\beta^2+5242880)x^6\\
&+\Big(15854469120\beta^6+33030144000\beta^4\\
&+5426380800\beta^2+106168320)x^4+(6606028800\beta^6\\
&-7785676800\beta^4-884736000\beta^2-56033280)x^2\\
&+707788800\beta^6-176947200\beta^4\\
&+1371340800\beta^2+152616960)t^6\\
&+-(6291456\beta(528\beta^4+120\beta^2+5)x^7\\
&+4718592\beta(1008\beta^4+1400\beta^2+115)x^5\\
&+29491200\beta\Big(112\beta^4-88\beta^2-5\Big)x^3\\
&+22118400\beta(31+48\beta^4-8\beta^2\Big)x)t^5\\
&+(-(519045120\beta^4+70778880\beta^2+983040)x^8\\
&+(990904320\beta^4+825753600\beta^2+22609920)x^6\\
&+(1032192000\beta^4-486604800\beta^2-9216000)x^4\\
&+(663552000\beta^4-66355200\beta^2+85708800)x^2\\
&-58060800\beta^4-294451200\beta^2-83808000)T^4\\
&+(-1310720\beta(44\beta^2+3)x^9\\
&+11796480\beta(12\beta^2+5)x^7\\
&+1474560\beta(140\beta^2-33)x^5\\
&+11059200\beta(20\beta^2-1)x^3\\
&-(58060800\beta^3+147225600\beta)x)t^3\\
&+(-(4325376\beta^2+98304)x^{10}\\
&+(13271040\beta^2+1843200)x^8+(25804800\beta^2\\
&-2027520)x^6+(41472000\beta^2-691200)x^4\\
&-(21772800\beta^2+18403200)x^2-1814400\beta^2-2268000)t^2\\
&+(-196608\beta x^{11}+737280\beta x^9+1843200\beta x^7\\
&+4147200\beta x^5-3628800\beta x^3-907200\beta x)t+14175,
\end{aligned}
$$

$$
\begin{aligned}
G_3=&\,1006632960\beta\left(4\beta^2+1\right)^4t^{10}x+100663296\left(4\beta^2+1\right)^5t^{11}\\
&+(125829120\left(36\beta^2+1\right)\left(4\beta^2+1\right)^3x^2-31457280\\
&\times\Big(48\beta^4+88\beta^2-5\Big)\left(4\beta^2+1\right)^2\Big)t^9\\
&+(1006632960\beta\left(12\beta^2+1\right)\left(4\beta^2+1\right)^2x^3\\
&-754974720\beta\left(4\beta^2+1\right)(16\beta^4\\
&+24\beta^2+1)x)t^8+(62914560(4\beta^2+1)\\
&\times(336\beta^4+56\beta^2+1)x^4\\
&-(42278584320\beta^6+52848230400\beta^4\\
&+7927234560\beta^2+94371840)x^2\\
&-3774873600\beta^6-2831155200\beta^4\\
&+2689597440\beta^2-342097920)t^7\\
&+(25165824\beta(1008\beta^4+280\beta^2+15)x^5\\
&-440401920\beta(12\beta^2+1)(4\beta^2+3)x^3\\
&-70778880\beta(80\beta^4+40\beta^2-19)x)t^6
\end{aligned}
$$

$$
\begin{aligned}
&+((5284823040\,\beta^4+880803840\beta^2+15728640)\,x^6\\
&-(6606028800\,\beta^4+3303014400\beta^2+82575360)\,x^4\\
&-(3538944000\,\beta^4+1061683200\beta^2-168099840)\,x^2\\
&-530841600\beta^4-619315200\beta^2-236666880)\,t^5+\\
&\left(62914560\beta\left(12\beta^2+1\right)x^7-330301440\beta\,(4\,\beta^2+1)\,x^5\right.\\
&-58982400\beta\,(20\,\beta^2+3)\,x^3-44236800\\
&\times\beta\,(12\,\beta^2+7)\,x)\,t^4+((70778880\,\beta^2+1966080)\,x^8\\
&-(165150720\,\beta^2+13762560)\,x^6\\
&-(221184000\,\beta^2+11059200)\,x^4\\
&-(199065600\,\beta^2+38707200)\,x^2\\
&+29030400\beta^2-3801600)\,t^3\\
&+(3932160\,\beta x^9-11796480\beta x^7\\
&-22118400\beta x^5-33177600\beta x^3+14515200\beta\,x)\,t^2\\
&+(98304\,x^{10}-368640x^8-921600x^6-2073600x^4\\
&+1814400x^2+453600)\,t,
\end{aligned}
$$

$$
\begin{aligned}
D_3=\;&4096x^{12}+6144x^{10}+34560x^8+149760x^6\\
&+54000x^4+48600x^2\\
&+201326592\beta\left(4\beta^2+1\right)^5t^{11}x+16777216\\
&\times\left(4\beta^2+1\right)^6t^{12}+\left(25165824\left(44\beta^2+1\right)\left(4\beta^2+1\right)^4x^2\right.\\
&+6291456\,(16\,\beta^4-72\beta^2+21)\,(4\,\beta^2+1)^3\,)\,t^{10}\\
&+(83886080\times\beta\,(44\,\beta^2+3)\,(4\,\beta^2+1)^3x^3\\
&\left.+62914560\beta\left(16\beta^4-56\beta^2+9\right)\left(4\beta^2+1\right)^2x\right)t^9\\
&+\left(15728640\left(528\beta^4+72\beta^2+1\right)\left(4\beta^2+1\right)^2x^4\right.\\
&+23592960\left(4\beta^2+1\right)\left(12\beta^2-1\right)\left(16\beta^4\right.\\
&\left.-40\beta^2-3\right)x^2+2264924160\beta^8+2264924160\beta^6\\
&\left.-1415577600\beta^4+3538944000\beta^2+244776960\right)t^8\\
&+\left(25165824\beta\left(4\beta^2+1\right)\left(528\beta^4+120\beta^2+5\right)x^5\right.\\
&+62914560\beta\left(192\beta^6-336\beta^4-60\beta^2+1\right)x^3\\
&\left.+70778880\beta\left(4\beta^2+5\right)\left(16\beta^4-8\beta^2+5\right)x\right)t^7\\
&+((15502147584\,\beta^6\\
&+5284823040\beta^4+440401920\beta^2+5242880)\,x^6\\
&+\left(5284823040\beta^6-6606028800\beta^4-707788800\beta^2\right.\\
&+3932160)\,x^4+\left(3963617280\beta^6+2123366400\beta^4\right.\\
&\left.-530841600\beta^2+221184000\right)x^2+613416960\beta^6\\
&\left.+884736000\beta^4+1282867200\beta^2+62668800\right)t^6\\
&+(6291456\,\beta\,(528\,\beta^4\\
&+120\beta^2+5)\,x^7+4718592\beta\,(336\,\beta^4\\
&-280\beta^2-15)\,x^5+17694720\beta\,(112\,\beta^4+40\beta^2-5)\,x^3\\
&\left.+4423680\beta\left(208\beta^4+200\beta^2+145\right)x\right)t^5\\
&+\left(\left(519045120\beta^4+70778880\beta^2+983040\right)x^8\right.\\
&+\left(330301440\beta^4-165150720\beta^2-2949120\right)x^6\\
&+5529600\left(4\beta^2+1\right)\left(28\beta^2-1\right)x^4\\
&+\left(575078400\beta^4+331776000\beta^2+80179200\right)x^2\\
&\left.+13824000\beta^4-37324800\beta^2+36806400\right)t^4+(1310720\beta\\
&\times(44\,\beta^2+3)\,x^9+11796480\beta\,(2\,\beta-1)\,(2\,\beta+1)\,x^7\\
&+4423680\beta\left(28\beta^2+3\right)x^5+3686400\beta\left(52\beta^2+15\right)x^3\\
&\left.+691200\beta\left(20\beta^2-27\right)x\right)t^3+\left(\left(4325376\beta^2+98304\right)x^{10}\right.\\
&+\left(4423680\beta^2-368640\right)x^8+\left(15482880\beta^2\right.\\
&+552960)\,x^6+\left(35942400\beta^2+3456000\right)x^4\\
&\left.+\left(5184000\beta^2-2332800\right)x^2+777600\beta^2+1490400\right)t^2\\
&+\left(196608\beta x^{11}+245760\beta x^9+1105920\beta x^7+3594240\beta x^5\right.\\
&\left.+864000\beta x^3+388800\beta x\right)t\;+\;2025,
\end{aligned}
$$

$$
u\,[3]=q\,[3]\exp\left[2\mathrm{i}\beta\int\left|q\,[3]\right|^2dx\right],
$$

$$
\int\left|q\,[3]\right|^2dx=\frac{H_3}{D_3},
$$

$$
\begin{aligned}
H_3=\;&4096x^{13}+55296x^{11}+96000x^9+426240x^7\\
&+952560x^5++264600x^3+99225x+16777216\\
&\times\left(4\beta^2+1\right)^6t^{12}x+(\,201326592\beta\left(4\beta^2+1\right)^5x^2\\
&+201326592\beta\left(4\beta^2+1\right)^5)\,t^{11}\\
&+(\,25165824\left(44\beta^2+1\right)\left(4\beta^2+1\right)^4x^3\\
&+6291456\left(1424\beta^4+312\beta^2+29\right)\left(4\beta^2+1\right)^3x\,)\,t^{10}\\
&+(83886080\,\beta\,(44\,\beta^2+3)\,(4\,\beta^2+1)^3x^4\\
&+188743680\beta\,(\,240\beta^4\\
&+56\beta^2+7\,)\left(4\beta^2+1\right)^2x^2+62914560\left(16\beta^4-56\beta^2\right.\\
&\left.+9\,\right)\left(4\beta^2+1\right)^2\beta\,)\,t^9+(\,15728640\,(\,528\beta^4\\
&\left.+72\beta^2+1\right)\left(4\beta^2+1\right)^2x^5\\
&+7864320\left(4\beta^2+1\right)\\
&\times\left(17472\beta^6+5040\beta^4+620\beta^2+17\right)x^3\\
&\times(\,38503710720\beta^8-82292244480\beta^6\\
&-24064819200\beta^4+4293918720\beta^2\\
&+386334720)+x)\,t^8
\end{aligned}
$$

$$+\left(25165824\beta\left(4\beta^2+1\right)\left(528\beta^4+120\beta^2+5\right)x^6\right.$$
$$+62914560\beta\left(4416\beta^6+1680\beta^4+220\beta^2+11\right)x^4$$
$$+23592960\beta\left(1728\beta^6-2544\beta^4-540\beta^2+83\right)x^2$$
$$\left.+\;70778880\beta\left(4\beta^2+5\right)\left(16\beta^4-8\beta^2+5\right)\right)t^7$$
$$+((15502147584\,\beta^6+5284823040\beta^4$$
$$+440401920\beta^2+5242880)$$
$$\times x^7+(98297708544\,\beta^6+25102909440\beta^4$$
$$+1934622720\beta^2+35389440)\,x^5$$
$$+(25102909440\,\beta^6-24300748800\beta^4$$
$$\left.-3361996800\beta^2+236912640\right)x^3$$
$$+\left(8540651520\beta^6+5131468800\beta^4+221184000\beta^2\right.$$
$$+505036800)\,x)\,t^6+\left(6291456\beta\left(528\beta^4+120\beta^2+5\right)x^8\right.$$
$$+1572864\beta\left(15792\beta^4+2520\beta^2+95\right)x^6+29491200\beta$$
$$\times\left(336\beta^4-200\beta^2-15\right)x^4+4423680\beta\left(1552\beta^4\right.$$
$$\left.\left.+\;680\beta^2+85\right)x^2+4423680\beta\left(208\beta^4+200\beta^2+145\right)\right)t^5$$
$$+\left(\left(519045120\beta^4+70778880\beta^2+983040\right)x^9\right.$$
$$+\left(4482662400\beta^4+401080320\beta^2+4915200\right)x^7$$
$$+\left(2601123840\beta^4-858193920\beta^2-23224320\right)x^5$$
$$+\left(3052339200\beta^4+862617600\beta^2+58060800\right)x^3$$
$$+\left(1163980800\beta^4+626227200\beta^2+197164800\right)x)\,t^4$$
$$+\left(1310720\beta\left(44\beta^2+3\right)x^{10}\right.$$
$$+23592960\beta\left(24\beta^2+1\right)x^8$$
$$+1474560\beta\left(308\beta^2-47\right)x^6+40550400\beta\left(20\beta^2+3\right)x^4$$
$$\left.+147225600\beta\left(4\beta^2+1\right)x^2+691200\beta\left(20\beta^2-27\right)\right)t^3$$
$$+\left(\left(4325376\beta^2+98304\right)x^{11}+\left(47677440\beta^2+614400\right)x^9\right.$$
$$+\left(50872320\beta^2-2396160\right)x^7+\left(128839680\beta^2\right.$$
$$+6773760)\,x^5+\left(148953600\beta^2+11491200\right)x^3$$
$$\left.+\left(11145600\beta^2-3175200\right)x\right)t^2$$
$$+\left(196608\beta x^{12}+2408448\beta x^{10}\right.$$
$$+3317760\beta x^8+11335680\beta x^6+18835200\beta x^4$$
$$\left.+2980800\beta x^2+388800\beta\right)t.$$

References

[1] Garrett C and Gemmrich J 2009 Rogue waves *Phys. Today* **62** 62–3

[2] Solli D R, Ropers C, Koonath P and Jalali B 2007 Optical rogue waves *Nature* **450** 1054–7

[3] Akhmediev N, Dudley J M, Solli D R and Turitsyn S K 2013 Recent progress in investigating optical rogue waves *J. Opt.* **15** 060201

[4] Akhmediev N, Ankiewicz A and Taki M 2009 Waves that appear from nowhere and disappear without a trace *Phys. Lett.* A **373** 675–8

[5] Shats M, Punzmann H and Xia H 2010 Capillary rogue waves *Phys. Rev. Lett.* **104** 104503

[6] Efimov V B, Ganshin A N, Kolmakov G V, McClintock P V E and Mezhov-Deglin L P 2010 Rogue waves in superfluid helium *Eur. Phys. J. Spec. Top* **185** 181–93

[7] Bludov Y V, Konotop V V and Akhmediev N 2009 Matter rogue waves *Phys. Rev.* A **80** 033610

[8] Moslem W M, Shukla P K and Eliasson B 2011 Surface plasma rogue waves *Euro. Phys. Lett* **96** 25002

[9] Stenflo L and Marklund M 2010 Rogue waves in the atmosphere *J. Plasma Phys.* **76** 293–5

[10] Yan Z Y 2010 Financial rogue waves *Commun. Theor. Phys.* **54** 947–9

[11] Porsezian K and Nakkeeran K 2001 Optical solitons in presence of Kerr dispersion and self-frequency shift *Phys. Rev. Lett.* **76** 3955

[12] Shabat A and Zakharov V 1972 Exact theory of two-dimensional self-focusing and one-dimensional self-modulation of waves in nonlinear media *Sov. Phys. JETP* **34** 62–9

[13] Hirota R 1982 Bilinearization of soliton equations *J. Phys. Soc. Jpn.* **51** 323–31

[14] Akhmediev N, Eleonskii V M and Kulagin N E 1987 Exact first-order solutions of the nonlinear Schrödinger equation *Theor. Math. Phys.* **72** 809–18

[15] Ma Y C 1979 The perturbed plane-wave solutions of the cubic Schroedinger equation *Stud. Appl. Math.* **60** 43–58

[16] Peregrine D H and Austral J 1983 Water waves, nonlinear Schrödinger equations and their solutions *Math. Soc. B: Appl. Math.* **25** 16–43

[17] Akhmediev N, Ankiewicz A and Soto-Crespo J M 2009 Rogue waves and rational solutions of the nonlinear Schrödinger equation *Phys. Rev.* E **80** 026601

[18] Kedziora D J, Ankiewicz A and Akhmediev N 2011 Circular rogue wave clusters *Phys. Rev.* E **84** 056611

[19] Kedziora D J, Ankiewicz A and Akhmediev N 2012 Second-order nonlinear Schrödinger equation breather solutions in the degenerate and rogue wave limits *Phys. Rev.* E **85** 066601

[20] Ankiewicz A, Kedziora D J and Akhmediev N 2011 Rogue wave triplets *Phys. Lett.* A **373** 2782–5

[21] Guo B L, Ling L M and Liu Q P 2012 Nonlinear Schrödinger equation: generalized Darboux transformation and rogue wave solutions *Phys. Rev.* E **85** 026607

[22] Bindu S G, Mahalingam A and Porsezian K 2001 Dark soliton solutions of the coupled Hirota equation in nonlinear fiber *Phys. Lett.* A **286** 321–31

[23] Ankiewicz A, Soto-Crespo J M and Akhmediev N 2010 Rogue waves and rational solutions of the Hirota equation *Phys. Rev.* E **81** 046602

[24] Bandelow U and Akhmediev N 2012 Persistence of rogue waves in extended nonlinear Schrödinger equations: integrable Sasa-Satsuma case *Phys. Lett.* A **376** 1558–61

[25] Wang L H, Porsezian K and He J S 2013 Breather and rogue wave solutions of a generalized nonlinear Schrödinger equation *Phys. Rev.* E **87** 053202

[26] Wazwaz A M 2001 A reliable technique for solving linear and nonlinear Schrodinger equations by Adomian decomposition method *Bull. Inst. Math. Acad. Sinica* **29** 125–34

[27] Wazwaz A M 2006 Reliable analysis for the nonlinear Schrodinger equations with a cubic and a power law nonlinearities *Math. Comput. Model* **43** 178–84

[28] Wazwaz A M 2006 Exact solutions for the fourth order nonlinear Schrodinger equations with a cubic and a power law nonlinearities *Math. Comput. Model.* **43** 802–8
[29] Wazwaz A M 2008 A study on linear and nonlinear Schrodinger equations by the variational iteration method *Chaos Soliton Fract.* **37** 1136–42
[30] Kundu A 1984 Landau-Lifshitz and higher-order nonlinear systems gauge generated from nonlinear Schrödinger-type equations *J. Math. Phys.* **25** 3433–8
[31] Kodama Y 1985 Optical solitons in a monomode fiber *J. Stat. Phys.* **39** 597–614
[32] Johnson R S 1977 On the modulation of water waves in the neighbourhood of $kh \approx 1.363$ *Proc. Roy. Soc. London* A **357** 131–41
[33] Geng X G 1992 A hierarchy of nonlinear evolution-equations, its hamiltonian-structure and classical integrable system *Physica* A **180** 241–51
[34] Gu C H, Hu H S and Zhou Z X 2005 *Darboux Transformations in Integrable Systems: Theory and their Applications to Geometry* (New York: Springer-Verlag)
[35] Matveev V B and Salle M A 1991 *Darboux Transformations and Solitons* (Berlin-Heidelberg: Springer-Verlag)
[36] Geng X G and Tam H W 1999 Darboux transformation and soliton solutions for generalized nonlinear Schrödinger equations *J. Phys. Soc. Jpn.* **68** 1508–12
[37] Zhaqilao 2013 On Nth-order rogue wave solution to the generalized nonlinear Schrödinger equation *Phys. Lett.* A **377** 855–9
[38] Zhao L C, Liu C and Yang Z Y 2014 The rogue waves with quintic nonlinearity and nonlinear dispersion effects in nonlinear optical fibers *Commun. Nonlinear Sci. Numer. Simul.* (arXiv:1312.3397)
[39] Kedziora D, Ankiewicz A and Akhmediev N 2013 Classifying the hierarchy of nonlinear-Schrödinger-equation rogue-wave solutions *Phys. Rev.* E **88** 013207
[40] He J S, Zhang H R, Wang L H, Porsezian K and Fokas A S 2013 Generating mechanism for higher-order rogue waves *Phys. Rev.* E **87** 052914
[41] Li L J, Wu Z W, Wang L H and He J S 2013 High-order rogue waves for the Hirota equation *Ann. Phys.* **334** 198–211
[42] Ablowitz M J, Kaup D J, Newell A C and Segur H 1973 Nonlinear evolution equations of physical significance *Phys. Rev. Lett.* **31** 125–7
[43] Guo B L, Ling L M and Liu Q P 2013 High-order solutions and generalized Darboux transformations of derivative nonlinear Schrödinger equations *Stud. Appl. Math.* **130** 317–44
[44] Yang B, Zhang W G, Zhang H Q and Pei S B 2013 Generalized Darboux transformation and rogue wave solutions for the higher-order dispersive nonlinear Schrödinger equation *Phys. Scripta* **88** 065004
[45] Wang X, Li Y Q, Huang F and Chen Y 2014 Rogue wave solutions of AB system *Commun. Nonlinear Sci. Numer. Simul.* (arXiv:1312.6479)
[46] Wang X and Chen Y 2014 Rogue-wave pair and dark-bright-rogue wave solutions of the coupled Hirota equations *Chin. Phys.* B **23** 070203
[47] Wang X, Li Y Q and Chen Y 2014 Generalized Darboux transformation and localized waves in coupled Hirota equations (arXiv:1312.3436v2)
[48] Li B and Chen Y 2007 Symbolic computation and solitons of the nonlinear Schrödinger equation in inhomogeneous optical fiber media *Chaos Soliton Fract.* **33** 532–9
[49] Wang Q and Chen Y 2007 Symbolic computation of exact solutions expressible in rational formal hyperbolic and elliptic functions for nonlinear partial differential equations *Chaos Soliton Fract.* **31** 500–13
[50] Chen Y and Wang Q 2005 A new general algebraic method with symbolic computation to construct new doubly-periodic solutions of the (2+1)-dimensional dispersive long wave equation *Appl. Math. Comput.* **167** 919–29
[51] Li Y S 1999 *Soliton and Integrable System* (Shanghai: Shanghai Scientific and Technological Education Publishing House)
[52] Chen D Y 2006 *Soliton Introduction Science* (Beijing: Science Publishing House)
[53] Baronio F, Degasperis A, Conforti M and Wabnitz S 2012 Solutions of the vector nonlinear Schrödinger equations: evidence for deterministic rogue waves *Phys. Rev. Lett.* **109** 044102
[54] Baronio F, Conforti M, Degasperis A and Lombardo S 2013 Rogue waves emerging from the resonant interaction of three waves *Phys. Rev. Lett.* **111** 114101
[55] Kedziora D J, Ankiewicz A and Akhmediev N 2014 Rogue waves and solitons on a cnoidal background *Eur. Phys. J-Spec. Top* **223** 43–62
[56] Chan H N, Chow K W, Kedziora D J, Grimshaw R and Ding E 2014 Rogue wave modes for a derivative nonlinear Schrödinger model *Phys. Rev.* E **89** 032914